Silver Nanoparticle-Based Inkjet-Printed Metamaterial Absorber on Flexible Paper

Minyeong Yoo, *Student Member, IEEE*, Hyung Ki Kim, *Student Member, IEEE*, Sangkil Kim, Manos Tentzeris, *Fellow, IEEE*, and Sungjoon Lim, *Member, IEEE*

***Abstract*—In this letter, a novel, flexible inkjet-printed metamaterial absorber is proposed. The unit cell consists of a miniaturized Jerusalem-cross resonator and a completely conductive bottom. Because the conductive patterns are inkjet-printed using silver nanoparticle inks on paper, the proposed metamaterial absorber is flexible. It is also eco-friendly because it does not produce any chemical waste. In this letter, the working principle of the proposed miniaturized unit cell is explained, and parametric simulations are described. The inkjet-printing process is delineated, and the silver nanoparticle inks and paper used are characterized. The performance of the proposed absorber is demonstrated with a full-wave simulation and measurements at the *X*-band. The experimental results show that the absorption rate at 9.09 GHz is greater than 99% at the normal incidence. Angular and polarization insensitivity are also experimentally demonstrated.**

***Index Terms*—Absorber, electric *LC* resonator (ELC), flexibility and polarization independent, inkjet-printing technology, metamaterial, paper substrate, silver nanoparticle ink.**

I. Introduction

THE METAMATERIAL-BASED electromagnetic (EM) absorber is composed of periodic conductive patterns on a planar substrate. It has been studied widely since it was first introduced by Landy *et al.* [1] because it has several advantages, such as low cost, thin geometry, and easier extension to large areas. Many metamaterial absorbers show near-perfect absorptivity in spite of the absence of conventional EM absorbing material, such as ferrites, because metamaterials can independently adjust the effective permittivity and permeability. Therefore, perfect impedance matching between the metamaterial and air can be achieved, and the transmitted EM wave with zero reflection can be perfectly absorbed and dissipated by conductive and dielectric losses at strong resonance. Recently, various metamaterial absorbers have been researched for narrowband [1], [2], broadband [3], [4], polarization insensitivity [4], [5], wide angle [5], and active characteristics [6], [7] in microwave [1]–[6], terahertz [7], [8], infrared [9], [10], and optical regions [11]. In addition, metamaterial absorbers have been applied in diverse areas, such as bolometer [12], electromagnetic interference (EMI) [13], plasmonic sensor [10], and stealth technology [14]. Taking the characteristics of practical environments into consideration, many researchers have also investigated flexible metamaterial absorbers for curved, as well as flat, surfaces [14], [15].

In this letter, a flexible metamaterial absorber printed on a paper substrate by inkjet-printing technology is proposed. An inkjet-printed metamaterial absorber on a paper substrate has not been reported before, so this is the first attempt to demonstrate the potential of a metamaterial absorber that employs inkjet-printing technology. The proposed absorber exhibits near-perfect absorptivity at the resonant frequency. Near-perfect absorptivity is retained even when the flexible absorber is attached to a cylindrical object because of the angular insensitivity of the unit cell design, as well as the flexibility of the paper. The angular insensitive unit cell was inspired by [16]. In this work, a unit cell is miniaturized by increasing its effective capacitance and inductance. The proposed absorber is insensitive to polarization because of the structural symmetry of its unit cells. The miniaturization of the unit cell permits high absorptivity for incidence angles up to 40°. The proposed absorber is also flexible because of its paper substrate.

II. Design of the Inkjet-Printed Metamaterial Absorber

A. Structure of the Unit Cell

In general, metamaterials exhibit complex electric permittivity ε characteristics, as well as complex magnetic permeability under effective medium approximations [8]. When an EM wave enters the metamaterial normally, the intrinsic impedance ($Z(\omega)$) of the metamaterial is defined by ε and μ, as shown in the following equation:

$$Z(\omega) = \sqrt{\tilde{\mu}(\omega)/\tilde{\varepsilon}(\omega)}. \tag{1}$$

By making ε and μ identical, the intrinsic impedance $Z(\omega)$ can be perfectly matched to that of the free space, 377 Ω, which means that there is no reflected wave from the metamaterial

$$\Gamma(\omega) = \frac{Z(\omega) - Z_0}{Z(\omega) + Z_0}. \tag{2}$$

In addition, the metamaterials can have high absorptivity owing to the large imaginary parts of the refractive index n, which indicate the loss components. As a result, the perfect

Manuscript received March 05, 2015; accepted April 03, 2015. Date of publication April 07, 2015; date of current version September 03, 2015. This work was supported by the Low Observable Technology Research Center program of the Defense Acquisition Program Administration and Agency for Defense Development.

M. Yoo, H. K. Kim, and S. Lim are with the School of Electrical and Electronics Engineering, College of Engineering, Chung-Ang University, Seoul 156-756, Korea (e-mail: sungjoon@cau.ac.kr).

S. Kim and M. Tentzeris are with the ATHENA Group, School of Electrical and Computer Engineering, Georgia Institute of Technology, Atlanta, GA 30332 USA.

Color versions of one or more of the figures in this letter are available online at http://ieeexplore.ieee.org.

Digital Object Identifier 10.1109/LAWP.2015.2420712

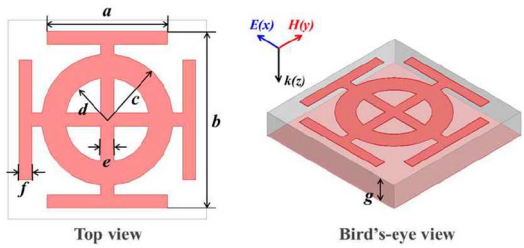

Fig. 1. Top view and bird's-eye view of the unit cell of the inkjet-printed metamaterial absorber: $a = 4.58$ mm, $b = 5.7$ mm, $c = 2.5$ mm, $d = 1.6$ mm, $e = 0.5$ mm, $f = 0.5$ mm, and $g = 1.19$ mm.

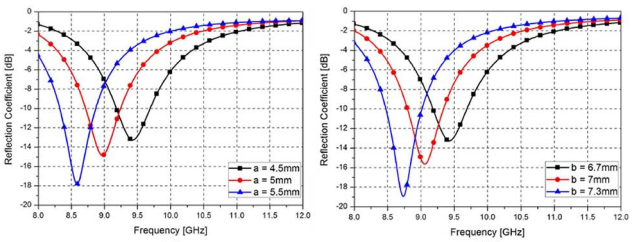

Fig. 2. Simulated reflection coefficients of the proposed absorber for different lengths of (a) the outermost arm a and (b) the crosswire b.

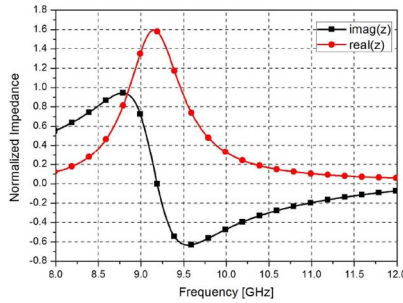

Fig. 3. Simulated normalized impedance of the proposed absorber.

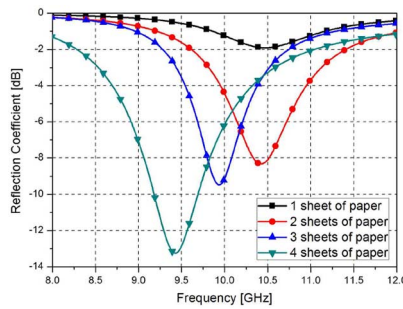

Fig. 4. Simulated reflection coefficients for different numbers of sheets of paper.

metamaterial absorber can be achieved by impedance matching between the metamaterial and air and large enough loss components, in spite of the thin configuration and the absence of EM-absorbing materials.

Fig. 1 shows the geometry of the proposed absorber's unit cell. The unit cell is made up of a Jerusalem-cross with an internal ring resonator on the top layer and a completely metal-covered bottom layer. The metallic pattern on the top layer is printed on a paper substrate using silver nanoparticle ink. Therefore, it has inductive and capacitive components and generates an electric resonance. Because the bottom layer of the proposed absorber is fully covered with a conductor, the transmission of the incident EM wave is zero.

B. Full-Wave Analysis

Because the modified Jerusalem-cross pattern has inductance L and capacitance C components, the LC resonance is generated at a specific frequency, defined by

$$f = \frac{1}{2\pi\sqrt{LC}}. \tag{3}$$

The resonance frequency depends on the L and C of the electric resonator on the top layer. Therefore, it can be shifted by changing the geometry of the top layer's metallic pattern. In particular, the outermost arm and crosswire (a and b, respectively, in Fig. 1) are the primary geometric parameters that determine C and L, respectively. To extend the unit cell design in [16] to the miniaturized unit cell design proposed here, a parametric study was performed for different values of a and b. For this study, a full-wave simulation was performed by applying the finite-element method (FEM), using a commercial high-frequency structure simulator (HFSS) from ANSYS, Inc., Pittsburgh, PA, USA. We used the master–slave boundary condition in the HFSS to analyze an infinite array of the a and b parameters for the proposed absorber. Fig. 2 shows the simulated reflection coefficients of the proposed absorber for different values of a and b. When a is decreased, C is also decreased, resulting from (3), in an increased resonance frequency, as shown in Fig. 2(a). Similarly, L is decreased when b is decreased, resulting in an increased resonance frequency, as shown in Fig. 2(b). Therefore, the miniaturization of the unit cell can be achieved by shifting to a higher resonance frequency.

Fig. 3 shows the impedance of the proposed absorber normalized to the impedance of the air. The proposed absorber exhibits resonance at 9.25 GHz with a real part that is near unity and an imaginary part of zero. This means that the proposed absorber has a good impedance matching to air at the resonance frequency, which leads to low reflection. In addition, because the real part of the normalized impedance is not perfectly matched to unity, it is possible to improve the performance by manipulating the geometry of the proposed absorber. To achieve perfect absorptivity with normalized impedance matched to unity, the transmitted wave must be attenuated by dielectric losses from the substrate. As shown in Fig. 4, as the substrate thickness increases, the reflection coefficients become lower and the frequency decreases.

III. Inkjet-Printing Process and Experimental Results

A. Inkjet-Printing Technology

When printed on the substrate, the silver nanoparticle ink forms a silver nanoparticle agglomeration containing polymers, dispersant, and surfactants necessary for uniform deposition by the inkjet. Owing to these impurities, the silver nanoparticle ink has poor conductivity immediately after printing, and a sintering process is therefore necessary to burn off the solvent and impurities. The sintering process also increases the bonding strength between the silver nanoparticle ink and the substrate,

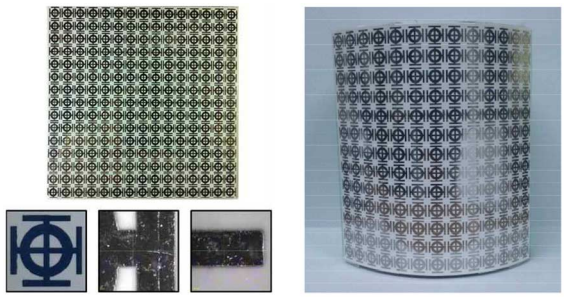

Fig. 5. (a) Flexible inkjet-printed absorber prototype and (b) absorber prototype coated on a polyethylene-terephthalate (PET) cylinder.

and melts the nanoparticles together to form a conductive layer. There are many sintering processes, such as thermal, laser, ultraviolet flash lamp, and microwave sintering. In this study, the thermal sintering process was used because of its simplicity and efficiency. A higher conductivity value can be achieved by increasing the sintering temperature.

For the inkjet printing process, a Dimatix DMP2800 inkjet printer with a Dimatix 10 pL cartridge (DMC-11610) was utilized. The angle of the printer head was set to print a pattern with a drop spacing of 20 μm, resulting in a print resolution of 1270 dots per inch. The ink that was used for the fabrication was DGP 40LT-15 C from Advanced Nano Products Company, Ltd. Once the desired pattern was formed, it was sintered in an oven for 2 hours at 130 °C to eliminate impurities. The conductivity of the silver used to produce the printed pattern ranges from 9×10^6 to 1.1×10^7 S/m, with a roughness of approximately 11 to 15 nm [17]. The conductivity value obtained is approximately 14.3% to 17.5% of the conductivity value of bulk silver (6.3×10^7 S/m), and similar to that of bulk iron (1.0×10^7 S/m).

B. Fabrication and Measurement Setup

The properties of a paper substrate in the microwave frequency range have been reported in [16]. The reported dielectric constant (ε_r) of a 0.23-mm-thick Kodak premium photo paper was 3.0, and the loss tangent ($\tan\delta$) was 0.05 at 0.8 to 10 GHz. The paper substrate has a relatively high $\tan\delta$, which is beneficial for microwave absorber designs, although it is detrimental to radio frequency circuit designs. Therefore, the high $\tan\delta$ is best utilized in a paper substrate applied as a microwave absorber. A prototype of the proposed absorber was printed on a paper, as shown in Fig. 5(a). The printed prototype consisted of 13×13 unit cells with a total area of 98.8×98.8 mm. The substrate consisted of four sheets of Kodak premium photo paper attached to each other with an adhesive, with a resulting total thickness of 1.19 mm. To demonstrate flexibility, the prototype absorber was coated on a polyethylene- terephthalate (PET) cylinder with a 4.56-cm radius. Fig. 5(b) shows a photograph of the absorber on the PET cylinder. It is known that this type of ink may crack when the polymer is folded because the polymer layer becomes hard after sintering. However, in this work, the ink did not crack because the proposed flexible absorber was not folded; instead, it was attached to the curved surface as shown in Fig. 5(b). The ink may be cracked when the absorber is repeatedly curved and flattened.

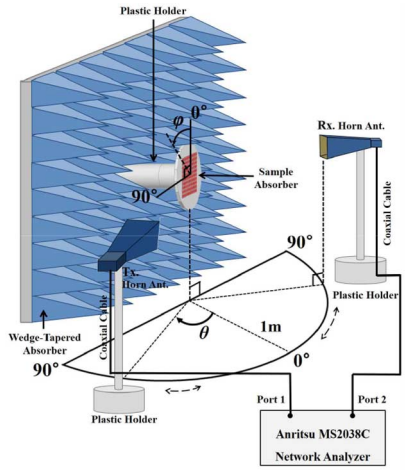

Fig. 6. Illustration of measurement setup.

To verify the performance of the proposed absorber, the fabricated prototype was measured using a bistatic radar cross section (RCS) measurement setup as in [4], as shown in Fig. 6. For the measurement, the prototype absorber was surrounded by a wedge-tapered absorber, and two horn antennas were placed 1 m away from the prototype absorber to satisfy the far-field condition. In addition, a time gating function in the vector network analyzer was applied to measure only the reflected signals from the prototype absorber. To measure the absorption rate for different polarization angles φ, the prototype absorber was rotated φ°. To measure the absorption rate at different incidence angles θ, the transmitting antenna was rotated θ°, and the receiving antenna was placed at an angle to satisfy Snell's law.

C. Discussion of Experimental Results

From the reflection $R(\omega)$ and transmission $T(\omega)$, we can obtain the absorption $A(\omega)$ from

$$A(\omega) = 1 - R(\omega) - T(\omega). \tag{4}$$

Because the bottom layer of the prototype absorber was completely covered with a metallic sheet, there was no transmission wave from the absorber. Therefore, we can neglect the transmission and obtain the absorption by measuring only the reflection coefficient.

The measured reflection coefficients for a vertically polarized incident wave on planar and curved surfaces are shown in Fig. 7, in which the full-wave simulation result from the HFSS is compared with the measurement results. When the absorber was on a planar surface, greater than 90% absorptivity was achieved from 8.8 to 9.46 GHz. In addition, greater than 90% absorptivity was achieved from 8.84 to 9.58 GHz, even when the absorber was coated on the curved surface of the PET cylinder.

To observe the absorptivity for different polarizations at normal incidence, one horn antenna was placed in front of the sample absorber, and the reflection coefficients were measured for different φ. The measured absorption ratios are plotted in Fig. 8(a). The plot indicates over 99% absorption at 9.09 GHz for all polarization angles.

The incident angle sensitivity of the proposed absorber was also investigated. The measured absorption ratios are shown in

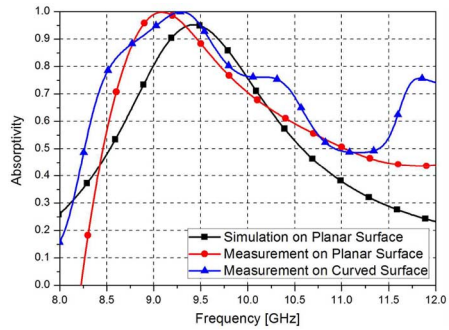

Fig. 7. Simulation and experimental absorptivity results for vertically polarized incident waves ($\varphi = 0°$, $\theta = 0°$) on planar and curved surfaces.

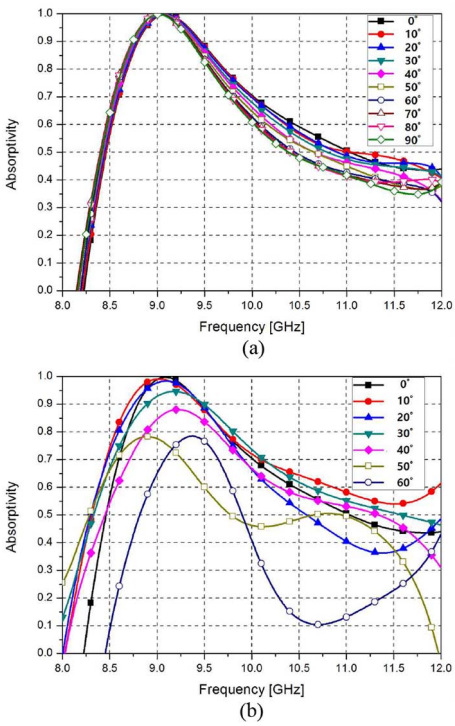

Fig. 8. Measured absorption ratio of the prototype absorber on a planar surface at different (a) polarization angles φ (varied from 0 to 90°) and (b) incidence angles θ (varied from 0 to 60°).

Fig. 8(b). The plot shows over 95% absorptivity at 9.09 GHz when θ is less than 30°. When θ was greater than 50°, the absorptivity decreased drastically. However, the proposed absorber maintained greater than 72% absorptivity at 9.09 GHz and greater than 78% absorptivity at the absorption peaks, which occurred at different frequencies for different θ.

IV. Conclusion

In this letter, we have proposed a novel flexible inkjet-printed metamaterial absorber. The proposed absorber was fabricated on a paper substrate using silver nanoparticle ink. Because of the high conductivity of the ink, the proposed absorber exhibits a high absorptivity, similar to a conventional metamaterial absorber. Furthermore, the proposed absorber is light and flexible because of its paper substrate, achieving over 90% absorptivity from 8.84 GHz to 9.58 GHz when coated on a PET cylinder. The proposed absorber exhibits polarization insensitivity and absorptivity of over 95% at 9.09 GHz for angles of incidence of less than 30°.

References

[1] N. Landy, S. Sajuyigbe, J. Mock, D. Smith, and W. Padilla, "Perfect metamaterial absorber," *Phys. Rev. Lett.*, vol. 100, no. 20, p. 207402, May 2008.

[2] J. Tak, Y. Lee, and J. Choi, "Design of a metamaterial absorber for ISM applications," *J. Electromagn. Eng. Sci.*, vol. 13, no. 1, pp. 1–7, Mar. 2013.

[3] J. Sun, L. Liu, G. Dong, and J. Zhou, "An extremely broad band metamaterial absorber based on destructive interference," *Opt. Express*, vol. 19, no. 22, pp. 21155–21162, Oct. 2011.

[4] M. Yoo and S. Lim, "Polarization-independent and ultrawideband metamaterial absorber using a hexagonal artificial impedance surface and a resistor-capacitor layer," *IEEE Trans. Antennas Propag.*, vol. 62, no. 5, pp. 2652–2658, May 2014.

[5] X. Shen *et al.*, "Polarization-independent wide-angle triple-band metamaterial absorber," *Opt. Express*, vol. 19, no. 10, pp. 9401–9407, May 2011.

[6] B. Zhu *et al.*, "Polarization modulation by tunable electromagnetic metamaterial reflector/absorber," *Opt. Express*, vol. 18, no. 22, pp. 23196–23203, Oct. 2010.

[7] H. Tao, A. Strikwerda, K. Fan, W. Padilla, X. Zhang, and R. Averitt, "MEMS based structurally tunable metamaterials at terahertz frequencies," *J. Infrared Millim. Terahertz Waves*, vol. 32, no. 5, pp. 580–595, May 2011.

[8] N. Landy *et al.*, "Design, theory, and measurement of a polarization-insensitive absorber for terahertz imaging," *Phys. Rev. B*, vol. 79, no. 12, p. 125104, Mar. 2009.

[9] X. Liu, T. Starr, A. Starr, and W. Padilla, "Infrared spatial and frequency selective metamaterial with near-unity absorbance," *Phys. Rev. Lett.*, vol. 104, no. 20, p. 207403, May 2010.

[10] N. Liu, M. Mesch, T. Weiss, M. Hentschel, and H. Giessen, "Infrared perfect absorber and its application as plasmonic sensor," *Nano Lett.*, vol. 10, no. 7, pp. 2342–2348, Jun. 2010.

[11] J. Hao *et al.*, "High performance optical absorber based on a plasmonic metamaterial," *Appl. Phys. Lett.*, vol. 96, no. 25, p. 251104, Jun. 2010.

[12] T. Maier and H. Brückl, "Wavelength-tunable microbolometers with metamaterial absorber," *Opt. Lett.*, vol. 34, no. 19, pp. 3012–3014, Oct. 2009.

[13] H. Kang and S. Lim, "High isolation transmitter and receiver antennas using high-impedance surfaces for repeater applications," *J. Electromagn. Waves Appl.*, vol. 27, no. 18, pp. 2281–2287, Sep. 2013.

[14] K. Iwaszczuk *et al.*, "Flexible metamaterial absorbers for stealth applications at terahertz frequencies," *Opt. Express*, vol. 20, no. 1, pp. 635–643, Jan. 2012.

[15] H. Tao *et al.*, "Highly flexible wide angle of incidence terahertz metamaterial absorber: Design, fabrication, and characterization," *Phys. Rev. B*, vol. 78, no. 24, p. 241103, Dec. 2008.

[16] Y. Cheng, H. Yang, Z. Cheng, and N. Wu, "Perfect metamaterial absorber based on a split-ring-cross resonator," *Appl. Phys. A*, vol. 102, no. 1, pp. 99–103, Jan. 2011.

[17] S. Kim *et al.*, "No battery required: Perpetual RFID-enabled wireless sensors for cognitive intelligence applications," *IEEE Microw. Mag.*, vol. 14, no. 5, pp. 66–77, Jul. 2013.